AD_____

Award Number: DAMD17-03-1-0037

TITLE: RAR Beta: Actions in Prostate Cancer

PRINCIPAL INVESTIGATOR: Yong Zhuang, Ph.D.

CONTRACTING ORGANIZATION: Weill Medical College of Cornell University
New York, NY 10021

REPORT DATE: April 2005

TYPE OF REPORT: Annual Summary

PREPARED FOR: U.S. Army Medical Research and Materiel Command
Fort Detrick, Maryland 21702-5012

REPORT DOCUMENTATION PAGE

Form Approved
OMB No. 0704-0188

1. REPORT DATE	2. REPORT TYPE	3. DATES COVERED
01-04-2005	Annual Summary	1 Apr 2004 – 31 Mar 2005

4. TITLE AND SUBTITLE
RAR Beta: Actions in Prostate Cancer

5a. CONTRACT NUMBER

5b. GRANT NUMBER
DAMD17-03-1-0037

5c. PROGRAM ELEMENT NUMBER

6. AUTHOR(S)
Yong Zhuang, Ph.D.

5d. PROJECT NUMBER

5e. TASK NUMBER

5f. WORK UNIT NUMBER

7. PERFORMING ORGANIZATION NAME(S) AND ADDRESS(ES)
Weill Medical College of Cornell
University
New York, NY 10021

8. PERFORMING ORGANIZATION REPORT NUMBER

9. SPONSORING / MONITORING AGENCY NAME(S) AND ADDRESS(ES)
U.S. Army Medical Research and Materiel Command
Fort Detrick, Maryland 21702-5012

10. SPONSOR/MONITOR'S ACRONYM(S)

11. SPONSOR/MONITOR'S REPORT NUMBER(S)

12. DISTRIBUTION / AVAILABILITY STATEMENT
Approved for Public Release; Distribution Unlimited

13. SUPPLEMENTARY NOTES

14. ABSTRACT

I have previously identified some RARβ targets genes. I found expression of one of the target gene, ELF3, is reduced in prostate cancer cells as compared to normal prostate epithelial cells. In the past year, I carried out transient transfection study to delineate how RA and RAR beta transcriptionally regulate ELF3 gene expression. I cloned a 1-kb ELF3 promoter into a luciferase reporter construct. Transient transfection assays showed that RA induced activity of the 1-kb ELF3 promoter (ELF3-luc) about 2.3 fold in F9 Wt cells. I also showed that retinol could induce the transcription of COUP-Tfs expression RARβ and its target genes in F9 teratocarcinoma cells at lower doses than RA. COUP-Tfs are nuclear receptors that have been shown to be required for the induction of RARβ transcription. They could play a role in the regulation of RARβ expression in prostate cancer.

15. SUBJECT TERMS
Prostate Cancer

16. SECURITY CLASSIFICATION OF:			17. LIMITATION OF ABSTRACT	18. NUMBER OF PAGES	19a. NAME OF RESPONSIBLE PERSON
a. REPORT	b. ABSTRACT	c. THIS PAGE			USAMRMC
U	U	U	UU	8	19b. TELEPHONE NUMBER *(include area code)*

Table of Contents

Introduction

Retinoids, a group of natural and synthetic analogues of vitamin A (retinol), can modulate cell growth and differentiation in vitro and in vivo (Gudas et al., 1994). An inverse relationship between retinoids levels and carcinogenesis has been observed over the last two decades. Vitamin A deficiency in experimental animals is associated with a higher incidence of cancer and with increased susceptibility to chemical carcinogens (Moon et al., 1994). Further, epidemiological studies showed that individuals with a lower dietary vitamin A intake are at a higher risk to develop cancer (Hong and Itri, 1994). Experimental models of carcinogenesis have demonstrated the efficacy of pharmacological levels of retinoids in preventing the development of cancers of the skin, oral cavity, lung, mammary gland, prostate, bladder, liver, and pancreas in animals exposed to carcinogenic agents (Moon et al., 1994). Thus, strong evidence exists that retinoids can prevent some types of cancers. Much in vitro and in vivo data indicate that retionoids play a role in the prevention of prostate cancer (Nanus and Gudas, 2000).

The biological effects of retinoids are mainly mediated by two classes of nuclear retinoid receptors: retinoic acid receptors (RARs) and retinoid X receptors (RXRs) (Mangelsdorf et al., 1994). The receptor RARβ is not expressed in a number of malignant tumors, including prostate cancer, lung carcinoma, squamous cell carcinoma of the head and neck, breast cancer, and esophageal carcinoma (Hu et al., 1991; Swisshelm et al., 1994; Zhang et al., 1994; Xu et al., 1994; Qiu et al., 1999). It has been suggested that the decrease in RARβ expression may lead to resistance to the growth inhibitory actions of retinoids. Indeed, transfection of RARβ into RARβ-negative cervical, breast, and lung cancer cells increased cell responsiveness to growth inhibition and induction of apoptosis by retinoids (Li et al., 1998; Si et al., 1996; Seewaldt et al., 1995; Liu et al., 1996; Weber et al., 1999). Stable expression of RARβ in a RARβ-negative prostate cancer cell line, PC-3, also potentiates the growth inhibitory effects of vitamin D3 analog and retinoids (Campbell et al., 1998).

In order to understand the function of the transcription factor RARβ, it is imperative that target genes regulated by RARβ are identified and analyzed. I have already successfully performed experiments to identify some of the target genes of RARβ in F9 cells by the use of subtractive hybridization and DNA expression micorarray techniques. By employing these two methods, I have identified many target genes, including transcription factors, protein tyrosine kinases, homeobox proteins, oncoproteins, ion channels, etc. Northern blot analysis was used to examine the regulation of the expression of these putative RARβ target genes by RA both in F9 Wt and F9 RARβ$_2$-/- cells. The regulation of these genes by RA was also examined by Northern blot analysis in F9 RARα-/- and RARγ-/- lines which were generated by homologous recombination in our laboratory.

Body

• **Carried out transient transfection experiment to delineate how ELF3 gene is transcriptionally regulated by RARβ and RA.** To delineate how the ELF3 gene is transcriptionally regulated by RARβ and RA, we amplified a 1kb promoter region of mouse ELF3 gene by PCR. We cloned this promoter fragment into a luciferase construct

PGL3 (ELF3-luc). We transfected this plasmid with or without other expression vectors into F9 wild type cells. Transfected cells were treated with RA or retinol for two days and luciferase activity was assayed. The result showed that RA induced activity of the 1-kb ELF3 promoter (ELF3-luc) about 2.3 fold in F9 Wt cells. In contrast, retinol has no effect on ELF3 promoter activity. Co-transfection of RARβ or COUP-TF2 (COUP) expression vectors did not enhance, but rather reduced RA effect (Figure 1). Additional analyses are underway to identify the sequences required for this transcriptional response.

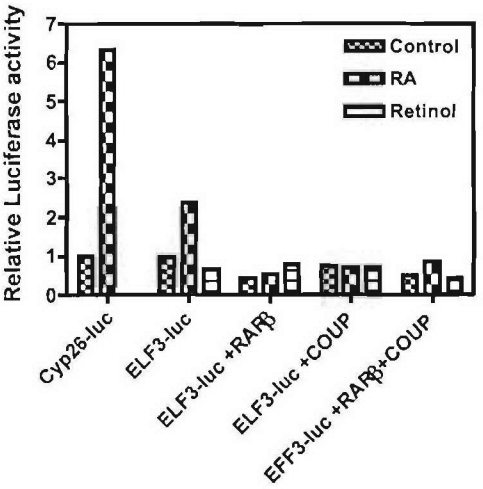

Figure 1. RA-induced transcription of a luciferase construct driven by ELF3 promoter. F9 Wt cells were incubated and transfected with 1 μg of indicated plasmids. Cells were incubated in culture medium with or without indicated retinoids for 2 days. Cells were lysed and cell extracts were assayed for luciferase activity.

• Examined the effects of retinol vs. RA on COUP-TFI and COUP-TFII mRNA expression in F9 Wild-type cells.

While we carried out previous experiments, we discovered that retinol could induce the transcription of RARβ and its target genes in F9 teratocarcinoma cells at lower doses than RA (data not shown). Since F9 cells do not metabolize retinol to RA, these data suggest that retinol can regulate gene expression without being metabolized to RA. To define the mechanism by which retinol stimulates RARβ mRNA expression we wanted to determine if retinol could induce COUP-TF expression, since a previous study suggested that COUP-TFI is required for the induction of RARβ transcription in human breast cancer cells (Lin et al., 2000). Thus, COUP-TFs could play a role in the regulation of RARβ expression in prostate cancer. Retinol treatment caused a dramatic induction of COUP-TFI and COUP-TFII mRNA at 6 h. In contrast, RA had no effect on COUP-TFI and COUP-TFII mRNA expression at 6 h (Figure 2A). Although both retinol and RA induced COUP-TFI and II mRNA at 24 h, the effect of RA was much smaller than that of retinol at the same concentration (data not shown). However, in contrast to what was observed for the COUP-TF genes, the effect of RA on the induction of Hoxa1 was much

stronger than that of retinol (Fig. 2A). Retinol induction of COUP-TF1 mRNA was completely blocked by treatment with actinomycin D (Figure 2B), indicating that transcription is required for retinol to induce the expression of the COUP-TFI gene in F9 cells. To examine if RARs are involved in COUP-TFI expression in F9 cells, we also compared the COUP-TFI mRNA expression in the F9 wild-type (Wt), RARα$^{-/-}$, RARβ$_2^{-/-}$, RARγ$^{-/-}$ cells. We found that COUP-TF1 mRNA level was comparable in F9 Wt, RARα$^{-/-}$ and RARβ$_2^{-/-}$ cells, but was induced more strongly by RA and Retinol in RARγ$^{-/-}$ cells. This suggests that RARγ represses COUP-TF1 expression in F9 cells (data not shown).

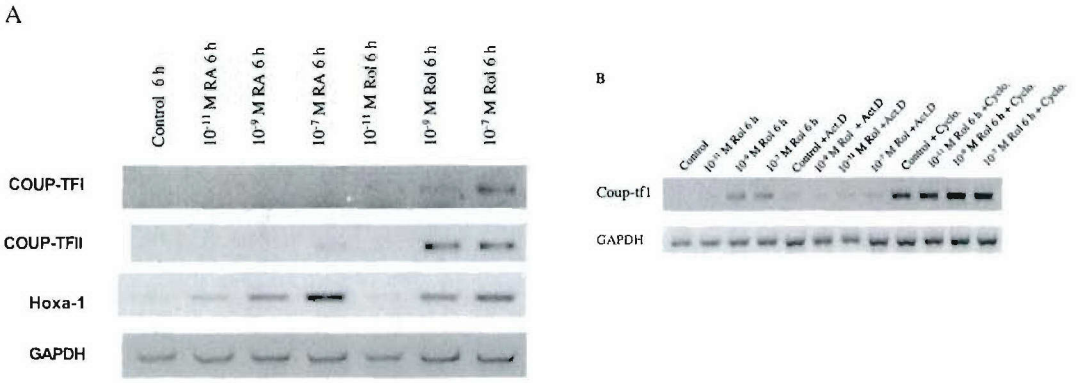

Figure 2. A. Effects of RA and retinol on the COUP-TF mRNA levels in F9 cells. F9 cells were treated with 1×10^{-11}, 1×10^{-9} or 1×10^{-7} M RA or retinol (Rol) and harvested at 6 hour. RNA was isolated and RT-PCR was used to detect the expression of COUP-TFs mRNA. GAPDH was used as a loading control. The experiment was repeated three times and one experiment is shown. **B. Effect of Actinomycin D (Act D) and Cycloheximide (Cyclo.) on expression of COUP-TFI mRNA.** F9 cells were cultured with or without retinol +/- actinomycin D (2 μg/ml) or cycloheximide for 6 hours. RNA was isolated and RT-PCR was used to detect the COUP-TFI mRNA. GAPDH was used as a sample loading control.

Key research Accomplishments

- I amplified a 1kb promoter region of mouse ELF3 gene by PCR. We cloned this promoter fragment into a luciferase construct PGL3.
- I carried out transient transfection experiments to delineate how RA and RARβ transcriptionally regulate ELF3 gene expression.
- I carried out RT-PCR analysis to examine effect of Retinol vs. RA on the COUP-Tfs gene expression, which are required for regulation of RARβ expression in cells and could be involved in reduced-expression of RARβ expression in prostate cancers.

Conclusions

I conclude that a 1-kb ELF3 promoter gave a response to RA in F9 Wt cells. Additional analyses are underway to identify the sequences required for this transcriptional response. In addition, I have shown that retinol treatment caused a dramatic induction of COUP-TFI and COUP-TFII mRNA at both 6 h and 24 h. In contrast, RA had no effect on COUP-TFI and COUP-TFII mRNA expression. I also show by actinomycin D experiments that transcription is required for retinol to induce the expression of the COUP-TFI gene.

References

Campbell, M. J., Park, S., Uskokovic, M. R., Dawson, M. I. And Koeffler, H. P. (1998) Expression of retinoic acid receptor-beta sensitizes prostate cancer cells to growth inhibition mediated by combination of retinoids and a 19-nor hexafluoride vitamin D3 analog. Endocrinology 139: 1972-1980

Gudas, L. J., Sporn, M. B. and Roberts, A. B. (1994) Cellular biology and biochemistry of the retinoids. In *the Retinoids* (Sporn, M. B., Roberts, A. B. and Goodman, D. S., eds) pp. 443-520, Raven Press, New York

Hong, W. K. and Itri, L. M. (1994) Retinoids and human cancer. In *The Retinoids* (Sporn, M. B., Roberts, A. B. and Goodman, D. S., eds) pp. 597-658, Raven Press, New York

Hu, L., Crowe, D. L., Rhenwald, J. G., Chambon, P. and Gudas, L. (1991) Abnormal expression of retinoic acid receptors and keratin 19 by human oral and epidermal squamous cell carcinoma cell lines. Cancer research. 51: 3972-3981

Li, Y., Dawson, M.I., Agadir, A., Lee, M. O., Jong, L., Hobbs, P. D. and Zhang, X. K. (1998) Regulation of RARb expression by RAR- and RXR-selective retinoids in human lung cancer cell lines: effect on growth inhibition and apoptosis induction. International Journal of Cancer 75: 88-95

Liu, Y., Lee, M. O., Wang, H. G., Li. Y., Hashimoto, Y., Klaus, M. Reed, J. C. and Moon, R. C., Mehta, R. C. and Rao, K. J. V. N. (1994) Retinoids and cancer in experimental animals. In *the Retinoids* (Sporn, M. B., Roberts, A. B. and Goodman, D. S., eds) pp. 573-595, Raven Press, New York

Mangelsdorf, D. J., Umesono, K. and Evans, R. M. (1994) The Retinoid receptors. In *the Retinoids* (Sporn, M. B., Roberts, A. B. and Goodman, D. S., eds) pp. 319-350, Raven Press, New York

Nanus, D. M. and Gudas, L. J. (2000) Retinoids and prostate cancer. The Prostate Journal 2: 68-73

Qiu, H., Zhang, W., EI-Naggar, A. K. et al., (1999) Loss of retinoic acid receptor-b expression is an early event during esophageal carcinogenesis. American Journal of Pathology 155: 1519-1523

Seewaldt, V. L., Johnson, B. S., Parker, M. B., Collins, S. J. and Swisshelm, K. (1995) Expression of retinoic acid receptor b mediates retinoic acid-induced growth arrest and apoptosis in breast cancer cells. Cell Growth & Differentiation 6: 1077-1088

Si, S. P., Lee, X., Tsou, H. C., Buchsbaum, R., Tibaduiza, E. and Peacocke, M. (1996) RAR beta 2-mediated growth inhibition in Hela cells. Experimental Cell Research 223, 102-111

Swisshelm, K., Ryan, K., Lee, X., Tsou, H. C., Beacocke, M. and Sager, R. (1994) Down-regulation of retinoic acid receptor b in mammary carcinoma cell lines and its up-regulation in senescing normal mammary epithelial cells. Cell Growth and Differentiation 5: 133-141

Weber, E., Ravi, R. K., Knudsen, E. S., Williams, J.R., Dillehay, L. E., Nelkin, B. D., Kalemkerian, G. Pl, Feramisco, J. R. and Mabry, M. (1999) Retinoic acid-mediated growth inhibition of small cell lung cancer cells is associated with reduced myc and increased p27Kip1 expression. International Journal of Cancer 80: 935-943

Xu, X-C., Ro, J. Y., Lee, J. S., Shin, D. M., Hong, W. K. and Lotan, R. (1994) Differential expression of nuclear retinoid receptors in normal, premalignant and malignant head and neck tissues. Cancer Research 54: 3580-3587

Zhang, X. K., Liu, Y., Lee, M. O. and Pfahl, M. (1994) A specific defect in the retinoic acid receptor associated with human lung cancer cell lines. Cancer Research 54: 5663-5669

Lin, B., Chen, G. Q., Xiao, D., Kolluri, S. K., Cao, X., Su, H., and Zhang, X. K. (2000). Orphan receptor COUP-TF is required for induction of retinoic acid receptor beta, growth inhibition, and apoptosis by retinoic acid in cancer cells. *Mol Cell Biol* **20,** 957-70.

THE JOURNAL OF BIOLOGICAL CHEMISTRY
Vol. 279, No. 38, Issue of September 17, pp. 40076–40083, 2004
Printed in U.S.A.

Activated Polyamine Catabolism Depletes Acetyl-CoA Pools and Suppresses Prostate Tumor Growth in TRAMP Mice*

Received for publication, May 28, 2004
Published, JBC Papers in Press, July 13, 2004, DOI 10.1074/jbc.M406002200

Kristin Kee‡, Barbara A. Foster‡, Salim Merali§, Debora L. Kramer‡, Mary L. Hensen‡, Paula Diegelman‡, Nicholas Kisiel‡, Slavoljub Vujcic‡, Richard V. Mazurchuk¶, and Carl W. Porter‡‖

From the Departments of ‡Pharmacology and Therapeutics and ¶Cancer Biology, Roswell Park Cancer Institute, Buffalo, New York 14263 and the §Department of Medical and Molecular Parasitology, New York University School of Medicine, New York, New York 10010

The enzyme spermidine/spermine N^1-acetyltransferase (SSAT) regulates the catabolism and export of intracellular polyamines. We have previously shown that activation of polyamine catabolism by conditional overexpression of SSAT has antiproliferative consequences in LNCaP prostate carcinoma cells. Growth inhibition was causally linked to high metabolic flux arising from a compensatory increase in polyamine biosynthesis. Here we examined the *in vivo* consequences of SSAT overexpression in a mouse model genetically predisposed to develop prostate cancer. TRAMP (transgenic adenocarcinoma of mouse prostate) female C57BL/6 mice carrying the SV40 early genes (T/t antigens) under an androgen-driven probasin promoter were cross-bred with male C57BL/6 transgenic mice that systemically overexpress SSAT. At 30 weeks of age, the average genitourinary tract weights of TRAMP mice were ~4 times greater than those of TRAMP/SSAT bigenic mice, and by 36 weeks, they were ~12 times greater indicating sustained suppression of tumor outgrowth. Tumor progression was also affected as indicated by a reduction in the prostate histopathological scores. By immunohistochemistry, SV40 large T antigen expression in the prostate epithelium was the same in TRAMP and TRAMP/SSAT mice. Consistent with the 18-fold increase in SSAT activity in the TRAMP/SSAT bigenic mice, prostatic N^1-acetylspermidine and putrescine pools were remarkably increased relative to TRAMP mice, while spermidine and spermine pools were minimally decreased due to a compensatory 5–7-fold increase in biosynthetic enzymes activities. The latter led to heightened metabolic flux through the polyamine pathway and an associated ~70% reduction in the SSAT cofactor acetyl-CoA and a ~40% reduction in the polyamine aminopropyl donor S-adenosylmethionine in TRAMP/SSAT compared with TRAMP prostatic tissue. In addition to elucidating the antiproliferative and metabolic consequences of SSAT overexpression in a prostate cancer model, these findings provide genetic support for the discovery and development of specific small molecule inducers of SSAT as a novel therapeutic strategy targeting prostate cancer.

Although prostate cancer can be clinically managed in its early phases, the inability to control the more aggressive late stage disease has prompted the search for novel therapies. We became interested in the possibility that strategies targeting polyamine homeostasis may be effective against prostate cancer. The prostate has the highest level of polyamine biosynthesis of any tissue, and it is the only tissue in which polyamines are purposely synthesized for export. More particularly, massive amounts of polyamines are excreted by the prostate into semen. Thus, we reasoned that polyamine homeostasis may be altered in the prostate relative to other tissues and that tumors derived from this gland may exhibit atypical regulatory responses to polyamine analogues and inhibitors (1). An additional rationale for targeting polyamines in prostate cancer derives from a recent meta-analysis of four independent microarray data sets comparing gene expression profiles of benign and malignant patient prostate samples showing that polyamine metabolism was the most systematically affected of all biochemical and signaling pathways (2). Genes that supported polyamine biosynthesis were up-regulated, while those that detracted from biosynthesis were down-regulated. The findings agree with earlier clinical studies showing a significant increase in ornithine decarboxylase (ODC)[1] and *S*-adenosylmethionine (AdoMet) decarboxylase transcripts in human prostatic cancer relative to benign hyperplasia (3).

Polyamines have been targeted in anticancer strategies for some time (4). Various antagonists such as the ODC inhibitor α-difluoromethylornithine (DFMO), AdoMet decarboxylase inhibitor (SAM486), and the polyamine analogue N^1,N^{11}-diethylnorspermine have undergone clinical testing as therapeutic and/or preventive agents (5, 6). Recognizing the unique physiology of the prostate gland, Heston and collaborators (7, 8) have proposed that polyamine inhibitors may be particularly effective against prostate cancer. In support of this concept, Gupta *et al.* (9) have shown that DFMO is effective in depleting polyamine pools and in preventing development of prostate cancer in the transgenic adenocarcinoma of mouse prostate (TRAMP) model (10).

Targeting polyamines has traditionally involved interference with or down-regulation of polyamine biosynthesis with small molecule inhibitors or analogues, respectively. As an alterna-

* This work was supported in part by National Institutes of Health Grant CA-76428 and by Department of Defense Grant DAMD17-03-1-0024, Core Grant CA16056, and Predoctoral Training Grant CA10972. The costs of publication of this article were defrayed in part by the payment of page charges. This article must therefore be hereby marked "*advertisement*" in accordance with 18 U.S.C. Section 1734 solely to indicate this fact.

‖ To whom correspondence and requests for reprints should be addressed: Dept. of Pharmacology and Therapeutics, Roswell Park Cancer Inst., Elm and Carlton Sts., Buffalo, NY 14263. Tel.: 716-845-3002; Fax: 716-845-2353; E-mail: carl.porter@roswellpark.org.

[1] The abbreviations used are: ODC, ornithine decarboxylase; AcSpd, N^1-acetylspermidine; DFMO, α-difluoromethylornithine; GU, genitourinary; HPCE, high performance capillary electrophoresis; MR, magnetic resonance; Put, putrescine; AdoMet, *S*-adenosylmethionine; Spd, spermidine; Spm, spermine; SSAT, spermidine/spermine N^1-acetyltransferase; Tag, SV40 large T antigen; TRAMP, transgenic adenocarcinoma of mouse prostate; H&E, hematoxylin and eosin; PBS, phosphate-buffered saline; AcSpm, acetylspermine.

tive to blocking biosynthesis, we propose that activation of polyamine catabolism by inducing the rate-limiting enzyme spermidine/spermine N^1-acetylspermine transferase (SSAT) may offer distinct advantages. The approach derives from our studies of the polyamine analogue N^1,N^{11}-diethylnorspermine that, in addition to down-regulating ODC and AdoMet decarboxylase, very potently up-regulates SSAT in tumor cells and tissues (11–14). The latter was shown to occur to a greater degree in human tumor xenografts than in normal host tissues (15). Correlations between SSAT induction and growth inhibition have been repeatedly suggested by early work in a variety of tumor types (14, 16, 17). Recently that relationship was more precisely defined by the finding that SSAT-targeted small interfering RNA minimizes analogue-mediated enzyme induction and at the same time prevents polyamine pool depletion and apoptosis (18, 19).

We have previously reported that conditional overexpression of SSAT in MCF-7 breast carcinoma cells leads to polyamine pool depletion and growth inhibition (20). As a prelude to the present study, we showed that conditional enzyme overexpression in LNCaP prostate carcinoma cells causes growth inhibition that differed from that seen in MCF-7 cells in that it was not accompanied by polyamine pool depletion (21). Instead cells averted the latter by increasing polyamine biosynthesis at the levels of ODC and AdoMet decarboxylase activities causing heightened metabolic flux through the biosynthetic and catabolic pathways. In a critical experiment, it was shown that interruption of flux by blocking ODC activity prevented growth inhibition (21). Additional studies concluded that growth inhibition deriving from overexpression of SSAT was probably attributable to overproduction of pathway products such as acetylated polyamines or to depletion of polyamine precursor metabolites such as AdoMet and/or the SSAT cofactor acetyl-CoA (21). Whatever the downstream mechanism, these *in vitro* data suggest that activation of polyamine catabolism by selective induction of SSAT may constitute an effective antitumor strategy against prostate cancer.

The goal of the present study was to further validate the above concept by providing critical *in vivo* evidence based on a genetic approach. For this purpose, we utilized the TRAMP model that is genetically engineered to develop prostate cancer (10, 22, 23). Cross-breeding these mice with SSAT transgenic mice that systemically overexpress the enzyme (24) resulted in a profound suppression of prostate tumor outgrowth that may be related to consequences emanating from depletion of acetyl-CoA pools.

EXPERIMENTAL PROCEDURES

Materials—The polyamines putrescine (Put), spermidine (Spd), spermine (Spm), and acetylated polyamine N^1-acetylspermidine (Ac-Spd) were purchased from Sigma. Acetyl-CoA was also purchased from Sigma and solubilized as described by Liu *et al.* (25).

Breeding and Screening of Transgenic Animals—TRAMP mice (10), heterozygous for the transgene rat probasin-SV40 large T antigen (PB-Tag) (lineage of founder 8247; Jackson Laboratory, Bar Harbor, ME) were maintained in a pure C57BL/6 background. Mouse tail DNA was isolated using the DNeasy® tissue kit (Qiagen Inc., Valencia, CA). Genotyping of TRAMP animals was performed by PCR according to the Jackson Laboratory protocol.

We previously generated mice that systemically overexpressed SSAT under its endogenous murine gene promoter (24). These SSAT transgenic mice, in the CD2F1 genetic background (24), were backcrossed for >8 generations into C57BL/6, the same genetic background as the TRAMP mouse. The SSAT transgenic mice are characterized by pronounced hair loss by 3–4 weeks of age (24), making genotyping unnecessary. Since female SSAT transgenic mice are infertile and male mice have normal reproductive capabilities, the latter were cross-bred with female TRAMP mice to generate the bigenic mice used in this study.

Magnetic Resonance (MR) Imaging—Longitudinal analysis of prostate cancer progression in TRAMP mice using MR imaging has been reported by Hsu *et al.* (26). More specifically, it was used to assess tumor volume and to track tumor development in TRAMP and TRAMP/SSAT mice. High resolution MR imaging scans were performed using a General Electric CSI 4.7T/33-cm horizontal bore magnet (GE NMR Instruments, Fremont, CA) with upgraded radio frequency and computer systems. MR imaging data were acquired using a custom designed 35-mm radio frequency transceiver coil and a G060 removable gradient coil insert generating a maximum field strength of 950 milliteslas/m. Transaxial, T1-weighted images were acquired through the lower abdomen with a standard spin echo MR imaging sequence. Images were comprised of 20 × 1-mm thick slices with a 3.2× 3.2-cm field of view acquired with a 192 × 192 matrix to provide contiguous image data of the prostate tumor. Acquisition parameters consisted of an echo time/repetition time = 10/724 ms and 4 number of excitations.

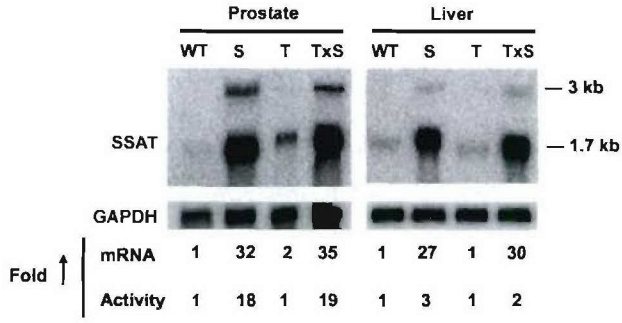

FIG. 1. **SSAT expression in the prostates and livers from SSAT transgenic mice.** Total RNA was isolated from the prostates and livers of littermates obtained from the TRAMP × SSAT cross and subjected to Northern blot analysis and enzyme activity assay (33, 39). Note the presence of a 3-kb heteronuclear SSAT RNA and a 1.7-kb mature SSAT mRNA. For quantitation, the 1.7-kb SSAT mRNA bands were scanned densitometrically and normalized to the glyceraldehyde-3-phosphate dehydrogenase (*GAPDH*) signal. Both SSAT mRNA and activity were expressed as -fold increase (*Fold* ↑) of wild-type tissue. SSAT mRNA was highly expressed in both prostate and liver of the SSAT (*S*) and the bigenic TRAMP/SSAT (*TxS*) mice but poorly expressed in the wild-type (*WT*) and TRAMP (*T*) animals. Northern blots are representative of those obtained during two experiments using 30 μg of total RNA/lane.

Pathology—Mouse genitourinary (GU) tracts consisting of bladder, urethra, seminal vesicles, ampullary gland, and the prostate were excised and weighed. The correlation of GU weight as a function of cancer progression in the TRAMP mouse is well documented by Kaplan-Lefko *et al.* (27). Once GU tracts were grossly examined and documented by fixed angle photography, the dorsal, lateral, ventral, and anterior lobes of the prostate as well as the seminal vesicles were microdissected and placed into multichamber cassettes for fixation in 4% paraformaldehyde for 4 h at 4 °C after which they were paraffin-embedded, sectioned at 5 μm, and stained with hematoxylin and eosin (H&E). H&E slides were reviewed by two experienced morphologists without knowledge of the genotype or age of the mice. Each prostatic lobe (dorsal, lateral, ventral, and anterior) was scored according to the grading system established by Gingrich *et al.* (28). The histological scores were then averaged and expressed as mean ± S.E.

Immunohistochemistry—Slides containing 5-μm sections were quenched with aqueous 3% hydrogen peroxide for 30 min and rinsed with PBS/T (500 μl/liter Tween 20) to remove endogenous peroxidases. Antigen retrieval involved continuous microwaving of the slides in 10 mM citrate buffer (pH 6.0) for 20 min. Cooled slides were washed for 5 min in PBS/T at room temperature and blocked with 0.03% casein in PBS/T for 30 min prior to the addition of primary antibodies. For anti-SV40 large T antigen staining, monoclonal anti-SV40 large T antigen antibody (catalog number 554149, BD Pharmingen) was used at a 1:400 dilution in a humidity chamber. Following overnight incubation at 4 °C, slides were washed with PBS/T and incubated for 30 min with secondary biotinylated anti-rabbit and anti-mouse immunoglobulins from the LSAB+ kit (DAKO, Carpinteria, CA) diluted according to the manufacturer's protocol. The slides were then washed with PBS/T and complexed with streptavidin (LSAB+ kit, DAKO, prediluted) for 30 min. Immunoreactive anti-SV40 large T antigen was detected by the application of the substrate 3,3′-diaminobenzidine tetrahydrochloride (DAKO) for 5 min. All sections were counterstained with hematoxylin.

Analytical Methods—Tissues were snap-frozen in liquid nitrogen, crushed into a fine powder in a mortar or a Bio-Pulverizer (BioSpec Products, Inc., Bartlesville, OK), and then sonicated on ice in Tris/

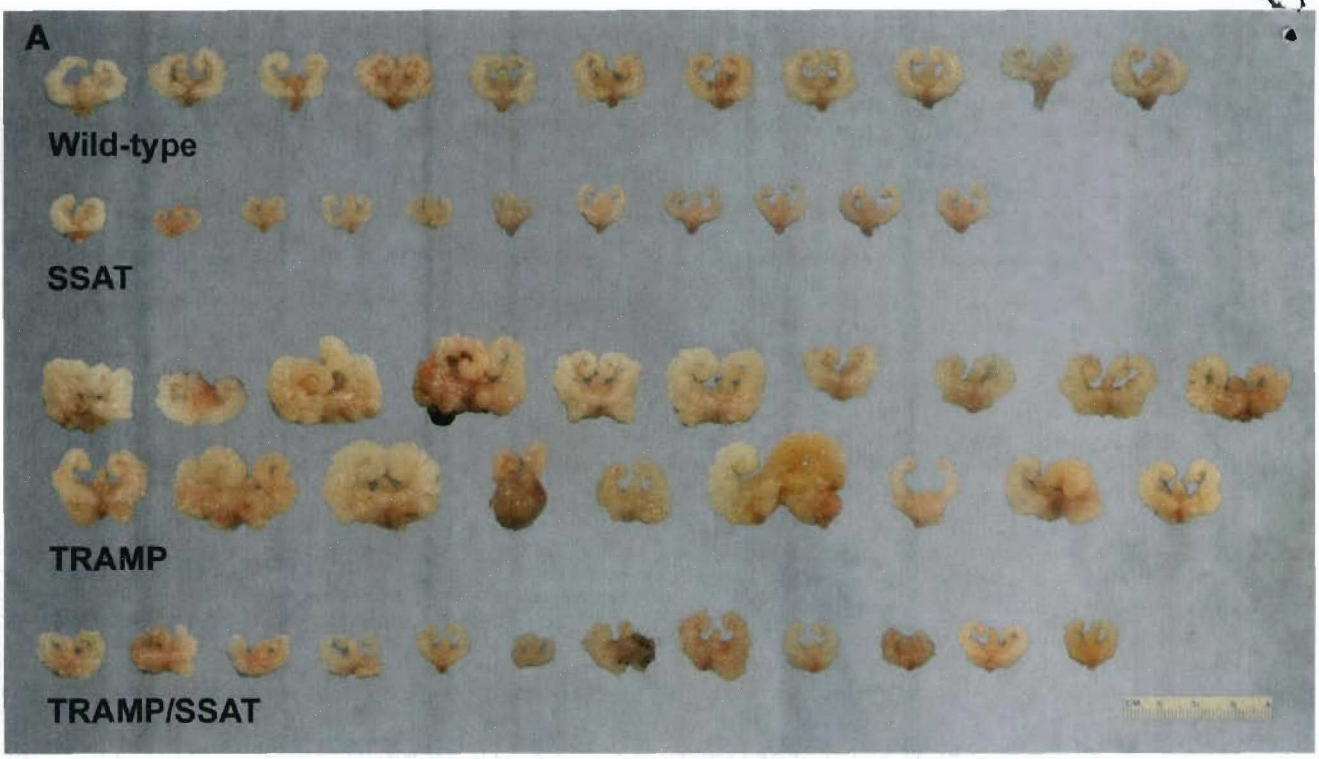

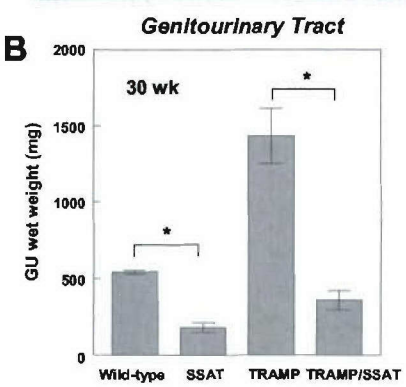

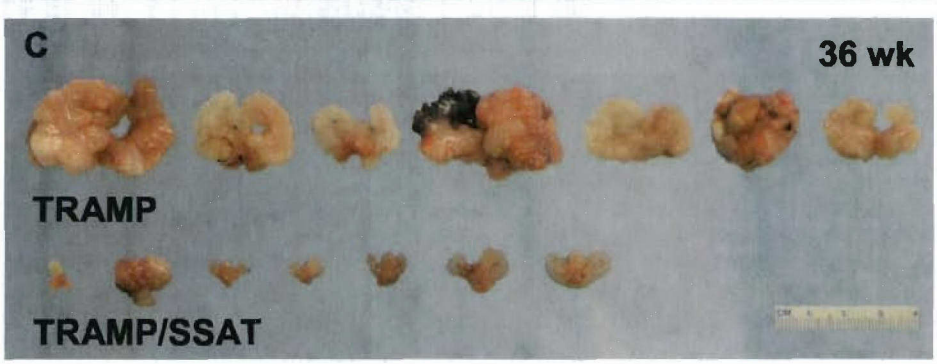

FIG. 2. **Comparison of GU tracts.** *A*, GU tracts of the four genetic cohorts deriving from the TRAMP × SSAT cross at 30 weeks. Note that the GU tracts of SSAT mice were smaller than those of wild-type mice and that the GU tracts of TRAMP/SSAT mice were much smaller and less variable in size and shape than those of TRAMP mice. *B*, GU tract weights at 30 weeks of four genetic cohorts deriving from the TRAMP × SSAT cross. The GU tracts of TRAMP/SSAT animals weighed less than TRAMP mice (*, $p < 0.0001$), and GU tracts of SSAT mice were also different from wild type (*, $p < 0.0001$) as determined by Student's unpaired t test. *C*, comparison of GU tracts for TRAMP and TRAMP/SSAT mice at 36 weeks of age. During the period of 30–36 weeks, the average TRAMP GU tract increased by 200%, while the average TRAMP/SSAT GU tract remained statistically the same (see Table I for detailed analysis).

EDTA buffer for polyamine enzyme activities and pool analysis. SSAT activity was assayed as described previously (29) and expressed as pmol of N^1-[^{14}C]acetylspermidine generated/min/mg of protein. Decarboxylase activities were determined by a CO_2 trap assay and expressed as pmol of CO_2 released/h/mg of protein (30). Polyamines and the acetylated derivatives of Spd and Spm were measured by high pressure liquid chromatography following methods reported by Kramer *et al.* (30). For Northern blot analysis, frozen tissues were crushed into a fine powder using a mortar and pestle after which total RNA was extracted with guanidine isothiocyanate (31) and purified by CsCl gradient centrifugation (32). RNA was loaded onto a gel at 30 μg/lane and subjected to Northern blot analysis following procedures described by Fogel-Petrovic *et al.* (33).

Acetyl-CoA Determinations—High performance capillary electrophoresis (HPCE) separation and quantitation of acetyl-CoA in tissue samples as recently described (21) was carried out following the method of Liu *et al.* (25). Tissues extracts were then analyzed on a Beckman P/ACE MDQ capillary electrophoresis system (Fullerton, CA) equipped with a photodiode array detector and an uncoated fused silica capillary electrophoresis column of 75-μm inner diameter and 60 cm in length with 50 cm from inlet to the detection window (Polymicro Technologies, Phoenix, AZ). Electrophoretic conditions were according to Liu *et al.* (25) with minor modifications as described previously (21). Data were collected and processed by Beckman P/ACE 32 Karat software version 4.0. Acetyl-CoA levels were expressed as nmol/g of tissue.

Statistics—Statistical significance (p value) was determined by Student's t test or analysis of variance with Fisher's protected least significant difference test at a 95% confidence level using a StatView computer program (SAS Institute Inc., Cary, NC).

RESULTS AND DISCUSSION

The goal of this study was to provide *in vivo* genetic validation for the concept that activating polyamine catabolism at the level of SSAT will give rise to an antitumor response due to homeostatic perturbations in polyamine metabolism. The effort was catalyzed by our recent reports showing that conditional overexpression of SSAT inhibits *in vitro* growth of both MCF-7 breast carcinoma cells (20) and LNCaP prostate carcinoma cells (21). Consistent with these findings, we now demonstrate that overexpression of SSAT markedly suppresses tumor outgrowth of early and advanced prostatic cancer in TRAMP mice. As will be discussed, this may be due to unusual sensitivity of

prostate-derived tumors to polyamine perturbations and/or to novel metabolic disturbances emanating from compensatory responses to activated polyamine catabolism.

SSAT-overexpressing transgenic male mice were cross-bred with female TRAMP mice to yield four cohorts of offspring: wild type, SSAT transgenic mice, and TRAMP and TRAMP/SSAT bigenics 15 weeks of age. Prostate and liver tissues were excised from wild-type, SSAT, TRAMP, and TRAMP/SSAT mice to confirm SSAT mRNA expression and enzyme activity. As shown in Fig. 1, prostate gland SSAT mRNA levels were elevated 32- and 35-fold in both SSAT and TRAMP/SSAT cohorts, respectively, relative to wild-type mice. Consistent with SSAT gene overexpression prostatic enzyme activity in both SSAT and TRAMP/SSAT mice was elevated by ~18-fold. SSAT mRNA in liver of SSAT and TRAMP/SSAT mice was increased 20- and 30-fold over wild-type mice, but unlike the prostate, enzyme activities were only increased 3- and 2-fold, presumably due to tissue-specific differences in translational control (24). The data confirm that overexpression of SSAT occurs in the prostate of transgene-bearing mice.

Longitudinal assessment of the prostate by MR imaging was used to monitor tumor appearance and development in representative TRAMP animals. GU tumors were first apparent at ~20 weeks of age in TRAMP animals. By 30 weeks, all TRAMP mice had visible prostate tumors that, with time, infiltrated the seminal vesicles as is typical in the pure C57BL/6 genetic background (10, 22, 27, 34). As observed using MR imaging and confirmed at necropsy, some TRAMP mice exhibited predominantly prostatic tumors, while the majority showed significant prostate tumors with seminal vesicle involvement. Both pathologies were reduced in the TRAMP/SSAT mice. On the basis of tumor size in TRAMP mice, the experimental end point was set at week 30.

The suppressive effect of SSAT overexpression on tumor outgrowth is apparent in comparisons of dissected GU tracts shown in Fig. 2*A*. Gross examination of both wild-type and SSAT animals revealed GU tracts that were generally uniform in size and shape. As graphed in Fig. 2*B*, GU tracts of the SSAT mice were significantly smaller (178 ± 30 mg) than those of the wild-type mice (504 ± 11 mg) despite close similarities in body weight (~29.7 ± 0.6 *versus* 28.5 ± 0.5 g, respectively). All of the TRAMP mice displayed visible evidence of prostatic tumors with variable involvement of the seminal vesicles. On the basis of weight, TRAMP GU tracts (1,435 ± 181 mg) were, on average, 4 times larger than those of TRAMP/SSAT mice (356 ± 62 mg). Taken together, the data indicate that SSAT overexpression effectively suppresses tumor outgrowth in the TRAMP model. Since by itself, the 30-week data may reflect a delay in tumor development as opposed to a sustained antitumor effect, we examined tumor size at a later time point. For this, 36 weeks was the longest time possible without encountering tumor excess. Relative to the 30-week data, the average GU tract weight in the TRAMP mice became 200% larger, while that in the TRAMP/SSAT mice at 36 weeks remained statistically unchanged. Thus, suppression of tumor outgrowth became even more exaggerated during the 30–36-week period. Although these findings suggest that the survival time of the TRAMP/SSAT mice would be significantly extended beyond that of the TRAMP mice, such studies were precluded by the strong tendency of the older bigenics to develop skin pathologies.

Histopathological analysis from littermates of the TRAMP and SSAT transgenic crosses at 30 weeks demonstrated that the prostate tumors of TRAMP mice were heterogeneous, ranging from high grade prostatic intraepithelial neoplasia (grade 3) to poorly differentiated adenocarcinoma (grade 6), while

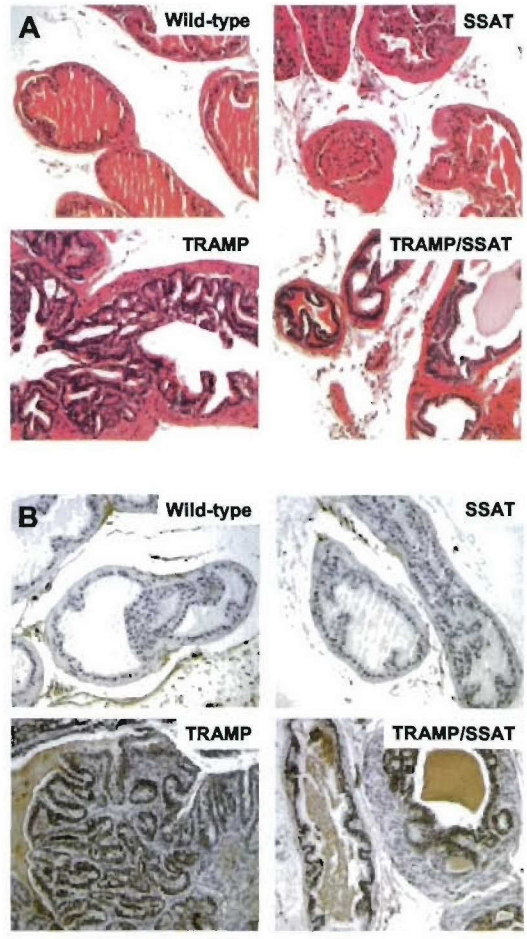

FIG. 3. **Sections of microdissected dorsal prostate.** *A*, representative H&E histological sections of the epithelium of the dorsal lobe of the mouse prostate. The four lobes of the prostate were graded and reported in Table I. TRAMP/SSAT prostates consistently displayed lower tumor grades than TRAMP prostates, which exhibited high grade prostatic intraepithelial neoplasia and well differentiated prostate carcinoma. The SSAT prostates showed normal epithelium. *B*, immunohistochemical detection of SV40 large T antigen. Expression of SV40 large T antigen was detected by immunohistochemistry in the epithelium of the dorsal lobe of 30-week-old TRAMP and TRAMP/SSAT mice but not in wild-type and SSAT mice. Large T antigen was also expressed in the glandular epithelial cells lateral, ventral, and anterior lobes (data not shown). Prostate tissues were analyzed from three mice per group. (H&E staining; microscopic magnification, 200×.)

tumors from TRAMP/SSAT mice were more homogeneous with a moderate range of prostatic intraepithelial neoplasia lesions (grades 2 and 3) and only rare evidence of well differentiated adenocarcinoma (grade 4) (Fig. 3*A*). Consistent with previous reports (28), disease in the TRAMP mouse was apparent in the dorsal, lateral, and ventral lobes with substantial seminal vesicle involvement, and it tended to be heterogeneous among mice. When all prostate lobes were averaged (Table I), the mean TRAMP/SSAT mouse grade (4.2) was significantly lower than that of the TRAMP mice (5.0) suggesting interference with disease progression. A similar trend was also seen at 36 weeks. Thus, while the major effect of SSAT overexpression is most obviously manifested as suppression of tumor outgrowth, there is also a delay in tumor progression. Because prostatic disease in the C57BL/6 background infiltrated the seminal vesicles, we derived an index to quantify overall GU disease. Thus, the average histological grades of the four lobes were averaged and then multiplied by the mean GU tract weight to derive a GU disease index for each cohort of animals (Table I). Based on this determination, the disease index at 30 weeks in

TABLE I
Genitourinary disease index of TRAMP/SSAT mice at 30 weeks

Mouse genotype	Age	No. of animals	Average prostate grade[a]			Average GU weight	GU disease index[c]	p value[d]
			Overall	Highest	Total[b]			
	wk				*g*			
TRAMP	30	15	2.1 ± 0.1	2.9 ± 0.1	5.0 ± 0.2	1.44 ± 0.18	7.44 ± 1.12	<0.0001
TRAMP/SSAT	30	10	2.0 ± 0.2	2.2 ± 0.2	4.2 ± 1.0	0.36 ± 0.06	1.51 ± 0.27	
TRAMP	36	8	2.8 ± 0.4	3.5 ± 0.4	6.3 ± 0.7	2.92 ± 0.81	22.57 ± 9.75	0.06
TRAMP/SSAT	36	6	2.5 ± 0.5	3.2 ± 0.5	5.6 ± 1.0	0.24 ± 0.12	2.08 ± 1.33	

[a] See Fig. 3*A* for representative histology of the prostate epithelium.
[b] The average prostate total grade for wild-type or SSAT mice was 2.0.
[c] GU disease index = (average overall grade + average highest grade) × average GU weight as determined per animal.
[d] Statistical significance (p value) was determined by analysis of variance with Fisher's protected least significant difference test.

TABLE II
Tissue polyamine metabolism in TRAMP × SSAT littermates

Data represent mean values ± S.E. where $n = 3$.

Mouse genotype	Tissue	Polyamine enzyme activities			Polyamine pools			
		SSAT	ODC	AdoMet DC	AcSpd[a]	Put	Spd	Spm
		pmol/min/mg protein	*pmol/h/mg protein*		*pmol/mg protein*			
Wild type	Prostate	5 ± 1	<20	60 ± 33	<40	140 ± 12	3,710 ± 402	7,990 ± 739
SSAT	Prostate	90 ± 20	190 ± 23	560 ± 81	2,440 ± 613	3,730 ± 805	7,350 ± 423	7,030 ± 458
TRAMP	Prostate	5 ± 1	<20	50 ± 19	<40	214 ± 34	4,830 ± 443	7,960 ± 881
TRAMP/SSAT	Prostate	90 ± 28	100 ± 21	370 ± 88	1,390 ± 187	3,520 ± 529	4,780 ± 858	5,280 ± 662
Wild type	Liver	15 ± 4	<20	120 ± 45	<40	<40	7,900 ± 368	8,510 ± 225
SSAT	Liver	50 ± 12	180 ± 32	940 ± 134	790 ± 210	4,260 ± 805	13,990 ± 794	5,060 ± 146
TRAMP	Liver	15 ± 2	<20	110 ± 75	<40	<40	9,510 ± 1389	10,840 ± 1,507
TRAMP/SSAT	Liver	30 ± 4	210 ± 15	550 ± 45	710 ± 241	4,520 ± 1,235	15,010 ± 2,376	5,770 ± 935

[a] AcSpm not detected in any samples.

the TRAMP/SSAT mice (1.51 ± 0.27) was found to be ~5-fold lower than that of the TRAMP mice (7.44 ± 1.12).

The suppression of tumor outgrowth seen here is consistent with a previous report showing that SSAT transgenic animals are more resistant to the development of skin papillomas under the two-stage skin carcinogenesis protocol (35). However, both studies differ from a report indicating that transgenic overexpression of SSAT in the mouse skin causes an increase in chemically induced tumor incidence (36). This is unexpected since our observations over the last 7 years find that spontaneous tumor formation was not increased in SSAT transgenic mice.[2] While the basis for this discrepancy is not immediately apparent, it is reasonable to consider that it may be due to promoter-dictated gene expression and/or to tissue-specific responses. For example, various tissues of the SSAT transgenic mouse adapt differently at the level of polyamine pool profiles (24) with some tissues, such as small intestine, displaying a greater effect on Spd than Spm pools and others, such as liver, showing a greater effect on Spm than Spd pools. Similarly different responses may be expected at the level of compensatory ODC induction, which as discussed below seems integral to the antitumor effect.

While several studies have undertaken genetic crosses with TRAMP mice, only one reports a negative effect on tumor outgrowth but not as great as that seen here. Abdulkadir *et al.* (37) showed that prostate tumorigenesis was impaired when Egr1-deficient mice were crossed with TRAMP mice. More particularly, the appearance of grossly evident tumors was delayed from 20 weeks in the TRAMP mouse to 35 weeks in the TRAMP × Egr1$^{-/-}$ mice. Of the reports in which TRAMP mice have been treated with various therapeutic and prevention agents, the most relevant involves chemoprevention of prostate carcinogenesis with the ODC inhibitor DFMO. Gupta *et al.* (9) found that DFMO in the drinking water of TRAMP mice from 8 to 28 weeks of age reduced the weight of the prostate and GU tracts by ~60% at 28 weeks while at the same time eliminating distant metastases. This is less than the 75% difference in GU weights seen here at 30 weeks. It is interesting to consider, however, that the Gupta study achieved the antitumor effect by pharmacologically *decreasing* polyamine biosynthesis, while the present study appears to have achieved a comparable effect by *increasing* polyamine biosynthesis secondary to SSAT overexpression as will be discussed below.

Before investigating the mechanistic basis for the tumor suppressive effect, we first determined that the SSAT overexpression did not interfere with expression of the driving oncogene in the TRAMP model Tag. Reduced expression of this transgene could originate systemically at the level of reduced androgen production, for example, or locally at the level of oncogene regulation. Both possibilities were eliminated by immunostaining for Tag protein levels in histological sections of 30-week TRAMP and TRAMP/SSAT prostates and tumors (Fig. 3*B*). Comparable levels of Tag were detected in the prostate epithelium of TRAMP and TRAMP/SSAT mice. Only minimal background staining was seen in the wild-type or SSAT transgenic mouse prostates or in appropriate controls lacking primary antibody. The findings confirm that Tag expression was not diminished in the TRAMP/SSAT mice and therefore was not responsible for the observed antitumor effects of SSAT.

To determine how polyamine-related events contribute to suppression of tumor outgrowth, we measured the activities of SSAT and the biosynthetic enzymes ODC and AdoMet decarboxylase as well as tissue polyamine and acetylated polyamine pools in both tumors and liver at 30 weeks. As shown in Table II, SSAT activity in the prostate tissue was elevated ~20-fold in both the SSAT and TRAMP/SSAT mice compared with wild-type and TRAMP mice. The more modest 2–3-fold enhancement of SSAT activity in the liver despite a 20-fold increase SSAT mRNA (38, 39) would seem to reflect tissue-specific translational control of this gene (38, 39). Increases in SSAT activity were accompanied by a profound (*i.e.* >10-fold) rise in biosynthesis at the level of ODC and AdoMet decarboxylase activities in both the prostate and the liver. As previously described in LNCaP cells (21), this represents a compensatory

[2] K. Kee, D. L. Kramer, and C. W. Porter, unpublished observations.

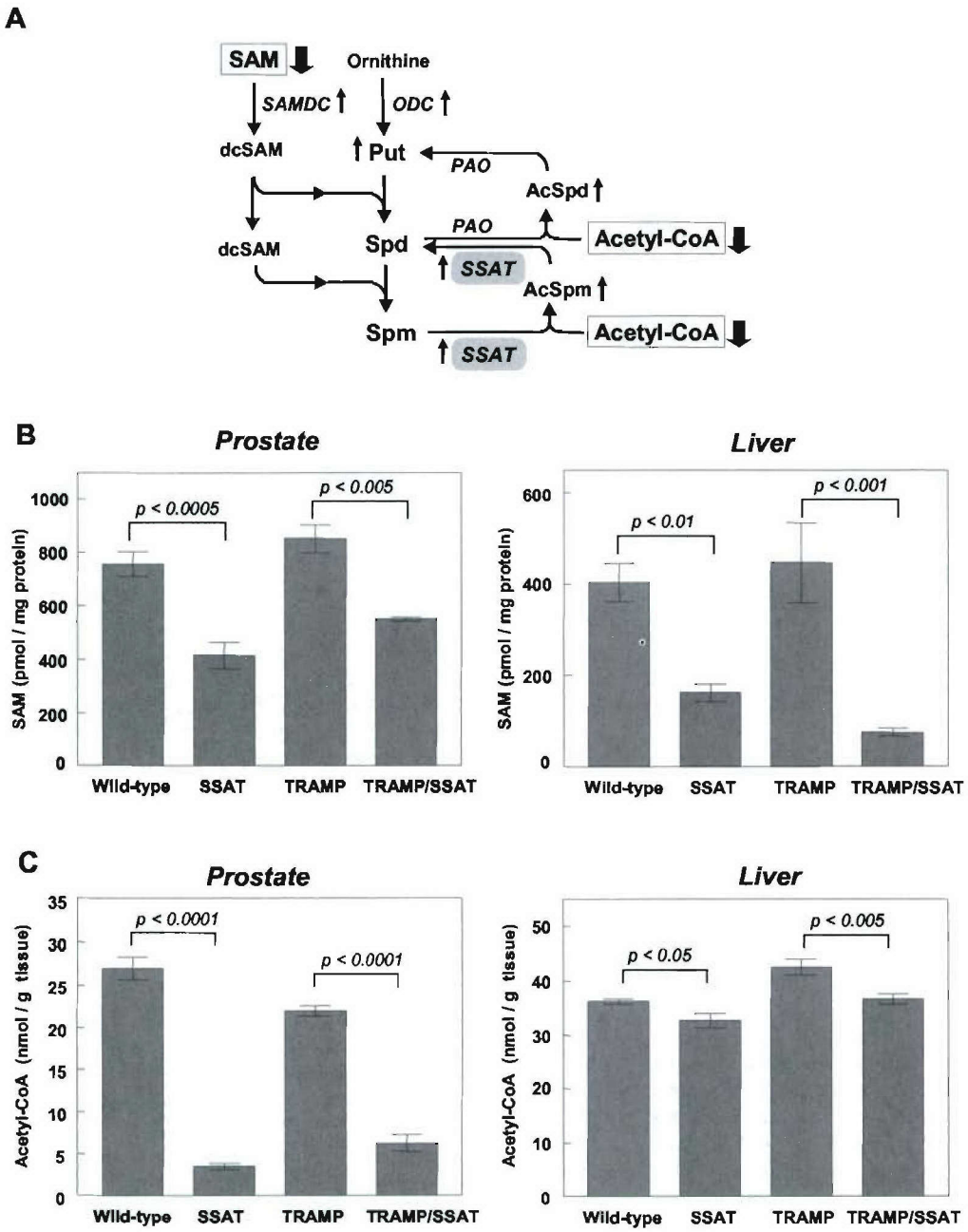

FIG. 4. **Downstream effects of SSAT overexpression.** *A*, metabolic consequences to SSAT overexpression. Activation of polyamine catabolism at the level of SSAT results in a compensatory increase in the activities of the polyamine biosynthetic enzymes ODC and AdoMet decarboxylase (*SAMDC*). This activated polyamine synthesis minimizes polyamine pool depletion despite massive production of AcSpd. At the same time, it gives rise to heightened metabolic flux through the biosynthetic and catabolic pathways (not shown). The possible downstream consequences connecting heightened metabolic flux to growth inhibition include overproduction of pathway products such as Put and AcSpd and/or depletion of critical metabolic precursors such as the aminopropyl donor AdoMet (*SAM*) and the SSAT cofactor acetyl-CoA, both of which are markedly decreased in SSAT transgenic and TRAMP/SSAT bigenic animals. *B*, AdoMet (*SAM*) levels in prostate and liver tissues of TRAMP/SSAT littermates as determined on tissue extracts by high performance liquid chromatography. Note that AdoMet pools were much lower (>40%) in the prostate and liver of SSAT and TRAMP/SSAT mice. *C*, acetyl-CoA levels in prostate and liver tissues of TRAMP × SSAT littermates as detected by HPCE. Note that during SSAT overexpression, there was significant reduction (~70%) of acetyl-CoA in the prostates of SSAT and TRAMP/SSAT mice but not in the livers. Data represents means ± S.E. where $n = 3$ animals per group. Statistical significance (p value) was determined by analysis of variance with Fisher's protected least significant difference test for pairwise comparisons. *PAO*, polyamine oxidase; *dcSAM*, decarboxylated AdoMet.

homeostatic response to activated polyamine catabolism. These changes in enzyme activities produced significant disturbances in tissue polyamine profiles particularly involving the acetylated polyamines. Although AcSpm remained undetectable, AcSpd increased from undetectable levels in the prostate and liver of wild-type and TRAMP mice to extraordinarily high levels in SSAT and TRAMP/SSAT mouse tissues. Another major finding was the accumulation of huge amounts of Put in both prostate and liver of SSAT-bearing mice, presumably due to the back conversion of Spd due to SSAT overexpression and to the forward conversion of ornithine due to high levels of ODC activity.

Despite the generation of large amounts of AcSpd, Spd pools remained relatively unaffected in the TRAMP/SSAT prostate tumors relative to TRAMP mice, while Spm decreased by ~33%, presumably due to back catabolism. This modest reduc-

tion in prostatic Spm pools hardly seems sufficient to account for the observed tumor growth suppression. As in LNCaP cells (21), the data suggest that the compensatory increase in polyamine biosynthesis and related metabolic flux may be playing a critical role in growth inhibition. More particularly, SSAT overexpression leads to massive acetylation and potential loss of cellular polyamines. To maintain a normal polyamine profile, the system responds by up-regulating ODC and AdoMet decarboxylase activities leading to a heightened metabolic flux through both arms of the pathway. Thus, ornithine is more rapidly converted to Spd and Spm, which in turn are more rapidly acted upon by SSAT to yield acetylated products. These findings are nearly identical to those elucidated in SSAT-overexpressing LNCaP prostate carcinoma cells (21) where activation of polyamine catabolism was also accompanied by increased polyamine biosynthesis. As a result, the Spd and Spm pools were unaffected despite massive production of acetylated polyamines. In a defining experiment, the relationship between this compensatory increase in ODC and growth inhibition in LNCaP cells was confirmed by the finding that growth inhibition is prevented by treatment with the ODC inhibitor DFMO. The compensatory increase in ODC and AdoMet decarboxylase activities in response to activated polyamine catabolism has been previously noted in various other tissues of the SSAT mouse (24) and, thus, is not unique to the prostate. The consequence of this effect, however, seems to be selective for both the male and female reproductive tracts since, as noted above, these are the only two organs that are underdeveloped in SSAT transgenic mice.

Guided by earlier findings in the LNCaP system (21), we examined the downstream consequences connecting heightened metabolic flux to growth inhibition or, in this case, suppression of tumor outgrowth (Fig. 1). Hence we focused on two classes of contributing events: toxic accumulation of metabolic products such as acetylated polyamines or depletion of critical metabolic precursors such as the aminopropyl donor AdoMet and/or the SSAT cofactor acetyl-CoA. Among the accumulated products, Put and AcSpd represent possible sources of tumor growth inhibition in bigenic mice and were not investigated further. On the precursor depletion side, the polyamine aminopropyl donor AdoMet and the SSAT cofactor acetyl-CoA were found to be significantly decreased in both SSAT and TRAMP/SSAT prostates. AdoMet pools were 40% lower in bigenic than in TRAMP mice (Fig. 4*B*). Even greater decreases were observed in the livers of SSAT transgenic mice. Although AdoMet is known to be critically involved in methylation reactions, it seems doubtful that the 40% pool reduction seen in the prostate tumors was growth-limiting since the liver showed a much greater decrease (85%) without obvious pathology and since the polyamines synthesized using AdoMet, Spd and Spm, were not decreased in the prostate tumors of bigenics. This does not, however, exclude the possibility that AdoMet is being preferentially diverted to polyamine biosynthesis at the expense of methylation reactions.

Attention was then focused on acetyl-CoA, which in addition to serving as a cofactor to SSAT is critically involved in fatty acid metabolism, cholesterol synthesis, and chromatin structure involving histone acetylation. Acetyl-CoA was impressively ~90% lower in prostates of SSAT mice than in wild-type mice and ~70% lower in TRAMP/SSAT mice than in TRAMP mice (Fig. 4*C*). By contrast, the acetyl-CoA pools in the livers of SSAT-bearing mice relative to non-SSAT-bearing mice were not similarly affected, consistent with the primary role of this organ in fat metabolism. Given the metabolic significance of acetyl-CoA, it is conceivable that the 70% reduction in pools seen in TRAMP/SSAT mice could impact negatively on tumor

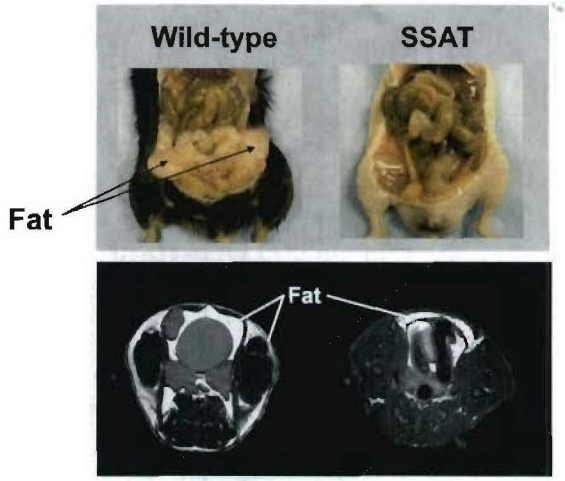

FIG. 5. **Abdominal fat stores in wild-type and SSAT transgenic mice at 30 weeks.** A comparison of dissected mice (*upper panel*) shows the presence of large abdominal/mesenteric fat deposits in wild-type animals (*left*) and the absence of similar deposits in the SSAT transgenic animals (*right*). Representative high resolution transaxial MR images (*lower panels*) of wild-type (*left*) and SSAT (*right*) mice are shown. Note the presence of abdominal and subdermal fat (seen as *bright areas*) in wild-type mice and the absence of similar deposits in SSAT transgenic mice.

growth. An indication that such perturbations may, in fact, interfere with fatty acid metabolism is strongly suggested by the observation that SSAT mice have markedly depleted abdominal and subdermal fat stores relative to wild-type mice (Fig. 5), an effect not previously reported in the original characterization of these mice (24).

As previously reported (21), acetyl-CoA was also found to be decreased during conditional overexpression of SSAT in LNCaP cells although not to the same extent as seen here. In cells, the effect correlated closely with growth inhibition, but it could not be causally linked to it. There are many previous reports suggesting a critical role for fatty acid metabolism in the prostate and prostate cancer. Intracellular lipidogenesis and *de novo* fatty acid metabolism at the level of fatty-acid synthase expression are known to be increased by androgens and have been implicated in aberrant growth of prostate tumor cells (40–42). The concept that tumors are more dependent than normal tissues on *de novo* fatty acid synthesis has led to the development of fatty-acid synthase inhibitors as anticancer agents for specific tumor types including prostate cancer (43–45). Recently Pflug *et al.* (45) demonstrated that the up-regulation of fatty-acid synthase expression plays a role in tumorigenesis in the TRAMP model and that prostate tumor cells are particularly sensitive to fatty-acid synthase inhibition. Since acetyl-CoA and malonyl-CoA are condensed by fatty-acid synthase to ultimately generate the 16-carbon polyunsaturated fatty acid palmitate, these findings imply a high dependence of prostate cancer on acetyl-CoA stores. In addition to playing a critical role in fatty acid metabolism, acetyl-CoA is also involved in controlling chromatin structure via histone acetylation. The latter opens chromatin structure and transcriptionally activates certain genes including some that mediate cell growth (46). Under conditions of limiting acetyl-CoA, such as those achieved in the prostate, it is possible that transcription of these growth-related genes may be repressed.

CONCLUSIONS

The present data provide unique insights into the *in vivo* biological potential of SSAT as a modulator of polyamine homeostasis, cellular metabolism, and tumor cell growth. These findings are reinforced by similar *in vitro* observations in

SSAT-overexpressing LNCaP cells (21). Both findings indicate that SSAT overexpression leads to up-regulation of ODC activity and to heightened metabolic flux through the polyamine pathway, which, in turn, has a significant impact on AdoMet and acetyl-CoA metabolism in both prostate cancer cells and tumors. To our knowledge, this has not been previously reported. The further possibility that these various metabolic perturbations may be responsible for the observed antitumor effect lends a novel dimension to SSAT induction that was not previously appreciated. More importantly, this study provides *in vivo* validation for the idea that pharmacological induction of SSAT may represent an effective therapeutic or preventive strategy. The finding that the normal prostate was underdeveloped in the SSAT transgenic mice would seem to indicate that such an approach may be best suited for prostate cancer in part because the organ itself appears to be uniquely dependent on acetyl-CoA as discussed above. The findings further suggest that a specific small molecule inducer of SSAT may find usefulness in targeting prostate cancer. There are a number of compounds that induce SSAT (5) with the best known being polyamine analogues such as N^1,N^{11}-diethylnorspermine (13, 47, 48). Although such analogues are potent inducers of SSAT, they also down-regulate polyamine biosynthesis, a response that would preclude heightened metabolic flux, which appears to be critical to the antiproliferative effect seen here (21). In addition, down-regulation of polyamine biosynthetic enzymes may account for the toxicity of polyamine analogues (12, 15, 16) since it is known that, unlike SSAT overexpression, which permits normal development except for hair loss and hypodeveloped reproductive tracts, ODC knock-out is embryonically lethal in mice (49). When taken together with the current data, these rationales present a compelling case for the discovery and development of a specific small molecule inducer of SSAT as a potential anticancer agent. In addition to having single agent potential, such a molecule may find application in augmenting the activity of certain clinically useful anticancer agents. For example, we have recently shown (50) that oxaliplatin and cisplatin potently up-regulate SSAT gene expression and that co-treatment with N^1,N^{11}-diethylnorspermine potentiates induction of SSAT enzyme activity as well as inhibition of cell growth. Presumably a specific SSAT inducer would behave similarly but with less host toxicity.

Acknowledgments—We gratefully acknowledge the suggestion of Dr. Paul Soloway to undertake this study and helpful discussions with Michael Moser. We also acknowledge Mehboob Shivji for assistance in the acetyl-CoA isolation protocol and greatly appreciate Mary Vaughan of the Roswell Park Institute histology core for help with histologic staining and immunohistochemistry.

REFERENCES

1. Mi, Z., Kramer, D. L., Miller, J. T., Bergeron, R. J., Bernacki, R., and Porter, C. W. (1998) *Prostate* **34,** 51–60
2. Rhodes, D. R., Barrette, T. R., Rubin, M. A., Ghosh, D., and Chinnaiyan, A. M. (2002) *Cancer Res.* **62,** 4427–4433
3. Bettuzzi, S., Davalli, P., Astancolle, S., Carani, C., Madeo, B., Tampieri, A., Corti, A., Saverio, B., Pierpaola, D., Serenella, A., Cesare, C., Bruno, M., Auro, T., and Arnaldo, C. (2000) *Cancer Res.* **60,** 28–34
4. Thomas, T., and Thomas, T. J. (2003) *J. Cell. Mol. Med.* **7,** 113–126
5. Seiler, N. (2003) *Curr. Drug Targets* **4,** 565–585
6. Seiler, N. (2003) *Curr. Drug Targets* **4,** 537–564
7. Heston, W. D., Watanabe, K. A., Pankiewicz, K. W., and Covey, D. F. (1987) *Biochem. Pharmacol.* **36,** 1849–1852
8. Heston, W. D. (1991) *Cancer Surv.* **11,** 217–238
9. Gupta, S., Ahmad, N., Marengo, S. R., MacLennan, G. T., Greenberg, N. M., and Mukhtar, H. (2000) *Cancer Res.* **60,** 5125–5133
10. Greenberg, N. M., DeMayo, F., Finegold, M. J., Medina, D., Tilley, W. D., Aspinall, J. O., Cunha, G. R., Donjacour, A. A., Matusik, R. J., and Rosen, J. M. (1995) *Proc. Natl. Acad. Sci. U. S. A.* **92,** 3439–3443
11. Libby, P. R., Bergeron, R. J., and Porter, C. W. (1989) *Biochem. Pharmacol.* **38,** 1435–1442
12. Casero, R. A., Jr., Ervin, S. J., Celano, P., Baylin, S. B., and Bergeron, R. J. (1989) *Cancer Res.* **49,** 639–643
13. Porter, C. W., Ganis, B., Libby, P. R., and Bergeron, R. J. (1991) *Cancer Res.* **51,** 3715–3720
14. Shappell, N. W., Miller, J. T., Bergeron, R. J., and Porter, C. W. (1992) *Anticancer Res.* **12,** 1083–1089
15. Porter, C. W., Bernacki, R. J., Miller, J., and Bergeron, R. J. (1993) *Cancer Res.* **53,** 581–586
16. Casero, R. A., Jr., Celano, P., Ervin, S. J., Porter, C. W., Bergeron, R. J., and Libby, P. R. (1989) *Cancer Res.* **49,** 3829–3833
17. McCloskey, D. E., and Pegg, A. E. (2000) *J. Biol. Chem.* **275,** 28708–28714
18. Chen, Y., Kramer, D. L., Li, F., and Porter, C. W. (2003) *Oncogene* **22,** 4964–4972
19. Chen, Y., Kramer, D. L., Jell, J., Vujcic, S., and Porter, C. W. (2003) *Mol. Pharmacol.* **64,** 1153–1159
20. Vujcic, S., Halmekyto, M., Diegelman, P., Gan, G., Kramer, D. L., Janne, J., and Porter, C. W. (2000) *J. Biol. Chem.* **275,** 38319–38328
21. Kee, K., Vujcic, S., Merali, S., Diegelman, P., Kisiel, N., Powell, C. T., Kramer, D. L., and Porter, C. W. (2004) *J. Biol. Chem.* **279,** 27050–27058
22. Gingrich, J. R., and Greenberg, N. M. (1996) *Toxicol. Pathol.* **24,** 502–504
23. Gingrich, J. R., Barrios, R. J., Kattan, M. W., Nahm, H. S., Finegold, M. J., and Greenberg, N. M. (1997) *Cancer Res.* **57,** 4687–4691
24. Pietila, M., Alhonen, L., Halmekyto, M., Kanter, P., Janne, J., and Porter, C. W. (1997) *J. Biol. Chem.* **272,** 18746–18751
25. Liu, G., Chen, J., Che, P., and Ma, Y. (2003) *Anal. Chem.* **75,** 78–82
26. Hsu, C. X., Ross, B. D., Chrisp, C. E., Derrow, S. Z., Charles, L. G., Pienta, K. J., Greenberg, N. M., Zeng, Z., and Sanda, M. G. (1998) *J. Urol.* **160,** 1500–1505
27. Kaplan-Lefko, P. J., Chen, T. M., Ittmann, M. M., Barrios, R. J., Ayala, G. E., Huss, W. J., Maddison, L. A., Foster, B. A., and Greenberg, N. M. (2003) *Prostate* **55,** 219–237
28. Gingrich, J. R., Barrios, R. J., Foster, B. A., and Greenberg, N. M. (1999) *Prostate Cancer Prostatic Dis.* **2,** 70–75
29. Bernacki, R. J., Oberman, E. J., Seweryniak, K. E., Atwood, A., Bergeron, R. J., and Porter, C. W. (1995) *Clin. Cancer Res.* **1,** 847–857
30. Kramer, D., Mett, H., Evans, A., Regenass, U., Diegelman, P., and Porter, C. W. (1995) *J. Biol. Chem.* **270,** 2124–2132
31. Chomczynski, P., and Sacchi, N. (1987) *Anal. Biochem.* **162,** 156–159
32. Ross, J. (1976) *J. Mol. Biol.* **106,** 403–420
33. Fogel-Petrovic, M., Shappell, N. W., Bergeron, R. J., and Porter, C. W. (1993) *J. Biol. Chem.* **268,** 19118–19125
34. Gingrich, J. R., Barrios, R. J., Morton, R. A., Boyce, B. F., DeMayo, F. J., Finegold, M. J., Angelopoulou, R., Rosen, J. M., and Greenberg, N. M. (1996) *Cancer Res.* **56,** 4096–4102
35. Pietila, M., Parkkinen, J. J., Alhonen, L., and Janne, J. (2001) *J. Investig. Dermatol.* **116,** 801–805
36. Coleman, C. S., Pegg, A. E., Megosh, L. C., Guo, Y., Sawicki, J. A., and O'Brien, T. G. (2002) *Carcinogenesis* **23,** 359–364
37. Abdulkadir, S. A., Qu, Z., Garabedian, E., Song, S. K., Peters, T. J., Svaren, J., Carbone, J. M., Naughton, C. K., Catalona, W. J., Ackerman, J. J., Gordon, J. I., Humphrey, P. A., and Milbrandt, J. (2001) *Nat. Med.* **7,** 101–107
38. Fogel-Petrovic, M., Vujcic, S., Brown, P. J., Haddox, M. K., and Porter, C. W. (1996) *Biochemistry* **35,** 14436–14444
39. Fogel-Petrovic, M., Vujcic, S., Miller, J., and Porter, C. W. (1996) *FEBS Lett.* **391,** 89–94
40. Swinnen, J. V., Esquenet, M., Goossens, K., Heyns, W., and Verhoeven, G. (1997) *Cancer Res.* **57,** 1086–1090
41. Swinnen, J. V., Ulrix, W., Heyns, W., and Verhoeven, G. (1997) *Proc. Natl. Acad. Sci. U. S. A.* **94,** 12975–12980
42. Swinnen, J. V., Vanderhoydonc, F., Elgamal, A. A., Eelen, M., Vercaeren, I., Joniau, S., Van Poppel, H., Baert, L., Goossens, K., Heyns, W., and Verhoeven, G. (2000) *Int. J. Cancer* **88,** 176–179
43. Kuhajda, F. P., Pizer, E. S., Li, J. N., Mani, N. S., Frehywot, G. L., and Townsend, C. A. (2000) *Proc. Natl. Acad. Sci. U. S. A.* **97,** 3450–3454
44. Pizer, E. S., Pflug, B. R., Bova, G. S., Han, W. F., Udan, M. S., and Nelson, J. B. (2001) *Prostate* **47,** 102–110
45. Pflug, B. R., Pecher, S. M., Brink, A. W., Nelson, J. B., and Foster, B. A. (2003) *Prostate* **57,** 245–254
46. Marks, P., Rifkind, R. A., Richon, V. M., Breslow, R., Miller, T., and Kelly, W. K. (2001) *Nat. Rev. Cancer* **1,** 194–202
47. Casero, R. A., Jr., Celano, P., Ervin, S. J., Wiest, L., and Pegg, A. E. (1990) *Biochem. J.* **270,** 615–620
48. Pegg, A. E., Pakala, R., and Bergeron, R. J. (1990) *Biochem. J.* **267,** 331–338
49. Pendeville, H., Carpino, N., Marine, J. C., Takahashi, Y., Muller, M., Martial, J. A., and Cleveland, J. L. (2001) *Mol. Cell. Biol.* **21,** 6549–6558
50. Hector, S., Porter, C. W., Kramer, D. L., Clark, K., Chen, Y., and Pendyala, L. (2004) *Mol. Cancer Ther.* **3,** 813–822